

TMC1 and TMC2 Proteins Are Pore-Forming Subunits of Mechanosensitive Ion Channels

Highlights

- Purified CmTMC1 and MuTMC2 proteins can incorporate into artificial liposomes
- CmTMC1 and MuTMC2 proteins are pore-forming ion channels
- CmTMC1 and MuTMC2 ion channels are mechanosensitive
- Deafness-related CmTMC1 mutants exhibit reduced or no ion channel activity

Authors

Yanyan Jia, Yimeng Zhao, Tsukasa Kusakizako, ..., Osamu Nureki, Motoyuki Hattori, Zhiqiang Yan

Correspondence

nureki@bs.s.u-tokyo.ac.jp (O.N.), hattorim@fudan.edu.cn (M.H.), zqyan@fudan.edu.cn (Z.Y.)

In Brief

Jia et al. used protein purification, functional reconstitution, and liposome recording to demonstrate that TMC1 and TMC2 proteins are pore-forming subunits of mechanosensitive ion channels, supporting TMC1 and TMC2 as hair cell transduction channels.

TMC1 and TMC2 Proteins Are Pore-Forming Subunits of Mechanosensitive Ion Channels

Yanyan Jia,^{1,4} Yimeng Zhao,^{2,4} Tsukasa Kusakizako,^{3,4} Yao Wang,² Chengfang Pan,¹ Yuwei Zhang,¹ Osamu Nureki,^{3,*} Motoyuki Hattori,^{2,*} and Zhiqiang Yan^{1,5,*}

¹State Key Laboratory of Medical Neurobiology and MOE Frontiers Center for Brain Science, Department of Neurosurgery at Huashan Hospital, Human Phenome Institute, Ministry of Education Key Laboratory of Contemporary Anthropology, Collaborative Innovation Center of Genetics and Development, Institute of Brain Science, Department of Physiology and Biophysics, School of Life Sciences, Fudan University, 2005 Songhu Road, Yangpu District, Shanghai 200438, China

²State Key Laboratory of Genetic Engineering, Collaborative Innovation Center of Genetics and Development, Multiscale Research Institute for Complex Systems, Department of Physiology and Biophysics, School of Life Sciences, Fudan University, Shanghai 200438, China

³Department of Biological Sciences, Graduate School of Science, The University of Tokyo, 7-3-1 Hongo, Bunkyo-ku, Tokyo 113-0033, Japan

⁴These authors contributed equally

⁵Lead Contact

*Correspondence: nureki@bs.s.u-tokyo.ac.jp (O.N.), hattorim@fudan.edu.cn (M.H.), zqyan@fudan.edu.cn (Z.Y.)

<https://doi.org/10.1016/j.neuron.2019.10.017>

SUMMARY

Transmembrane channel-like (TMC) 1 and 2 are required for the mechanotransduction of mouse inner ear hair cells and localize to the site of mechanotransduction in mouse hair cell stereocilia. However, it remains unclear whether TMC1 and TMC2 are indeed ion channels and whether they can sense mechanical force directly. Here we express TMC1 from the green sea turtle (CmTMC1) and TMC2 from the budgerigar (MuTMC2) in insect cells, purify and reconstitute the proteins, and show that liposome-reconstituted CmTMC1 and MuTMC2 proteins possess ion channel activity. Furthermore, by applying pressure to proteoliposomes, we demonstrate that both CmTMC1 and MuTMC2 proteins can indeed respond to mechanical stimuli. In addition, CmTMC1 mutants corresponding to human hearing loss mutants exhibit reduced or no ion channel activity. Taken together, our results show that the CmTMC1 and MuTMC2 proteins are pore-forming subunits of mechanosensitive ion channels, supporting TMC1 and TMC2 as hair cell transduction channels.

INTRODUCTION

Hearing, one of our primary senses, is essential for daily communication. In humans, the perception of sound begins with the organ of Corti in the inner ear, which harbors more than 16,000 hair cells (Gillespie and Müller, 2009; Schwander et al., 2010). In every hair cell, hair bundles are organized in rows of stereocilia of decreasing height (Gillespie and Müller, 2009; Schwander et al., 2010). Mechanotransduction channels, which convert the mechanical signals of sound into electrical signals, are thought to be localized in these hair bundles (Corey and Hud-

speth, 1979; Gillespie and Müller, 2009; Hudspeth and Corey, 1977; Schwander et al., 2010). Of all five of our senses defined by Aristotle—vision, taste, olfaction, touch, and hearing—the latter is the least well understood in terms of the molecular transduction mechanism. Indeed, the molecular identity of the auditory transduction ion channel at the heart of human sound perception is still not known.

Human genetics approaches that link human deafness to genes have been instrumental in understanding the molecular biology of hearing transduction. The transmembrane channel-like (TMC) 1 and 2 genes, first identified in deaf human patients, are essential for hearing in mice (Kawashima et al., 2011; Kurima et al., 2002; Vreugde et al., 2002). TMC1 and TMC2 are necessary for the mechanotransduction currents of hair cells, and TMC1 mutations can alter the properties of mechanosensitive currents in mice (Fettiplace, 2016; Kawashima et al., 2015; Marcotti et al., 2006; Pan et al., 2013, 2018). TMC1 and TMC2 are both expressed in hair cells and localized in stereocilia tips, where mechanotransduction occurs (Kurima et al., 2015). However, whether TMC1 and TMC2 proteins are ion channels and whether TMC1 and TMC2 can be gated by mechanical force remain unclear.

Here we took advantage of the expression screening of TMC proteins from different species. From a repertoire of 21 TMC1/2 proteins, we found that TMC1 from the green sea turtle *Chelonia mydas* (CmTMC1) and TMC2 from the budgerigar *Melopsittacus undulatus* (MuTMC2) showed a high level of expression in insect cells. We then reconstituted CmTMC1 and MuTMC2 in liposomes and found that these proteins exhibited robust channel activity. Successful reconstitution of CmTMC1 and MuTMC2 also allowed us to assess their mechanosensitivity. By applying pressure to the reconstituted channels, we showed that CmTMC1 and MuTMC2 proteins can directly respond to mechanical force. Although our study focuses primarily on CmTMC1 and MuTMC2, the strong evolutionary conservation of CmTMC1 and MuTMC2 with mouse TMC1 and TMC2 suggests that mammalian TMC1 and TMC2 are likely to be ion channels and to be mechanosensitive. Furthermore, we showed that

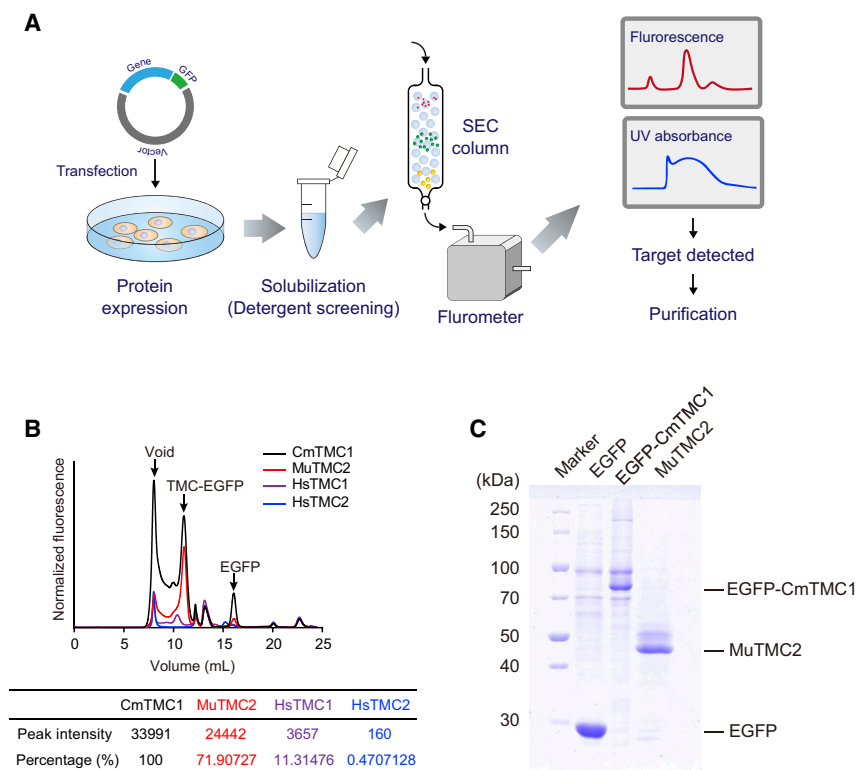


Figure 1. Expression and Purification of Target TMC Proteins

(A) Cartoon illustration of FSEC for TMC protein screening. Constructs of EGFP-tagged TMCs were transfected into Sf9 cells and solubilized in detergent. Through fluorescence detection of EGFP, the expression quantity and quality of TMC proteins were evaluated using gel filtration with fluorescence detection of the EGFP tag.

(B) FSEC profiles and quantification of the expression level of EGFP-tagged CmTMC1 (black), MuTMC2 (red), HsTMC1 (purple), and HsTMC2 (blue). The arrows indicate the elution positions of the void volume, CmTMC1-EGFP, MuTMC2, and free EGFP. The peak intensity of CmTMC1 is defined as 100%.

(C) SDS-PAGE analysis of TMC proteins and EGFP stained with Coomassie blue (12.5% acrylamide). Each lane contained 5 μ g of protein.

the mutants of CmTMC1 corresponding to the human hearing loss mutants exhibited reduced or no ion channel activity. Taking these results together with previous studies showing that TMC1/2 are expressed in hair cells and that TMC1/2 mutant mice have no mechanosensitive currents in hair cells, we propose that TMC1 and TMC2 proteins are pore-forming subunits of mechanosensitive ion channels involved in vertebrate hearing transduction.

RESULTS

Purification of TMC Proteins

In addition to the proteins found in humans and mice, TMC homologs in *Drosophila melanogaster* and *Caenorhabditis elegans* have been found in sensory neurons and are required for animal responses to physical stimuli (Chatzigeorgiou et al., 2013; Guo et al., 2016; Wang et al., 2016; Yue et al., 2018), but whether TMC proteins are ion channels remains unclear. Furthermore, TMC proteins are poorly trafficked to the cell membrane when expressed in cultured cells (Beurg et al., 2015; Kawashima et al., 2011; Labay et al., 2010; Wang et al., 2016; Zhao et al., 2014), hindering electrophysiological recording of TMC. To overcome this technical difficulty, we functionally reconstituted purified TMC1 and TMC2 proteins into liposomes to evaluate whether TMC proteins are indeed ion channels.

To identify suitable candidate TMC1 and TMC2 proteins for purification, we employed an ortholog screening approach. Because of the difficulty of expressing and purifying membrane proteins, ortholog screening is a common strategy to identify a

teins because ortholog screening by FSEC has been quite successful (Coleman et al., 2016; Hibbs and Gouaux, 2011; Kawate et al., 2009; Lee et al., 2014; Penmatsa et al., 2013; Sobolevsky et al., 2009).

As is standard for FSEC-based expression screening, we subcloned 21 TMC orthologs from different species (Table S1), including those from human and mouse, with EGFP tags and transiently expressed them in Sf9 cells (Figure 1A). The TMC-expressing cells were solubilized with detergents and applied to a size-exclusion chromatography column attached to a fluorimeter (Figure 1A). FSEC-based expression screening enabled us to rapidly evaluate the expression of TMC orthologs without extra protein purification steps because of the high sensitivity and specificity of GFP fluorescence. The solubilized TMC proteins are relatively monodisperse but also show significant void peaks and EGFP peaks (Figure 1B).

Although we did not find a high level of expression of human and mouse TMC proteins, we found that CmTMC1 and MuTMC2 exhibited high levels of expression (Figure 1B). Both CmTMC1 and MuTMC2 show high sequence identity and similarity to human TMC1 and human TMC2, respectively (CmTMC1, 72% sequence identity and 85% sequence similarity to human TMC1; MuTMC2, 66% sequence identity and 76% sequence similarity to human TMC2; Figure S1). Notably, hair cells of both birds and reptiles have tip links that link mechanical stimulus-responsive stereocilia arranged in a height gradation to adaptation currents (Crawford et al., 1991; Manley and Köppl, 2008; Ohmori, 1985; Pickles et al., 1989; Ricci and Fettiplace, 1997; Tsuprun et al., 2004), which is highly similar to the situation observed in mammals.

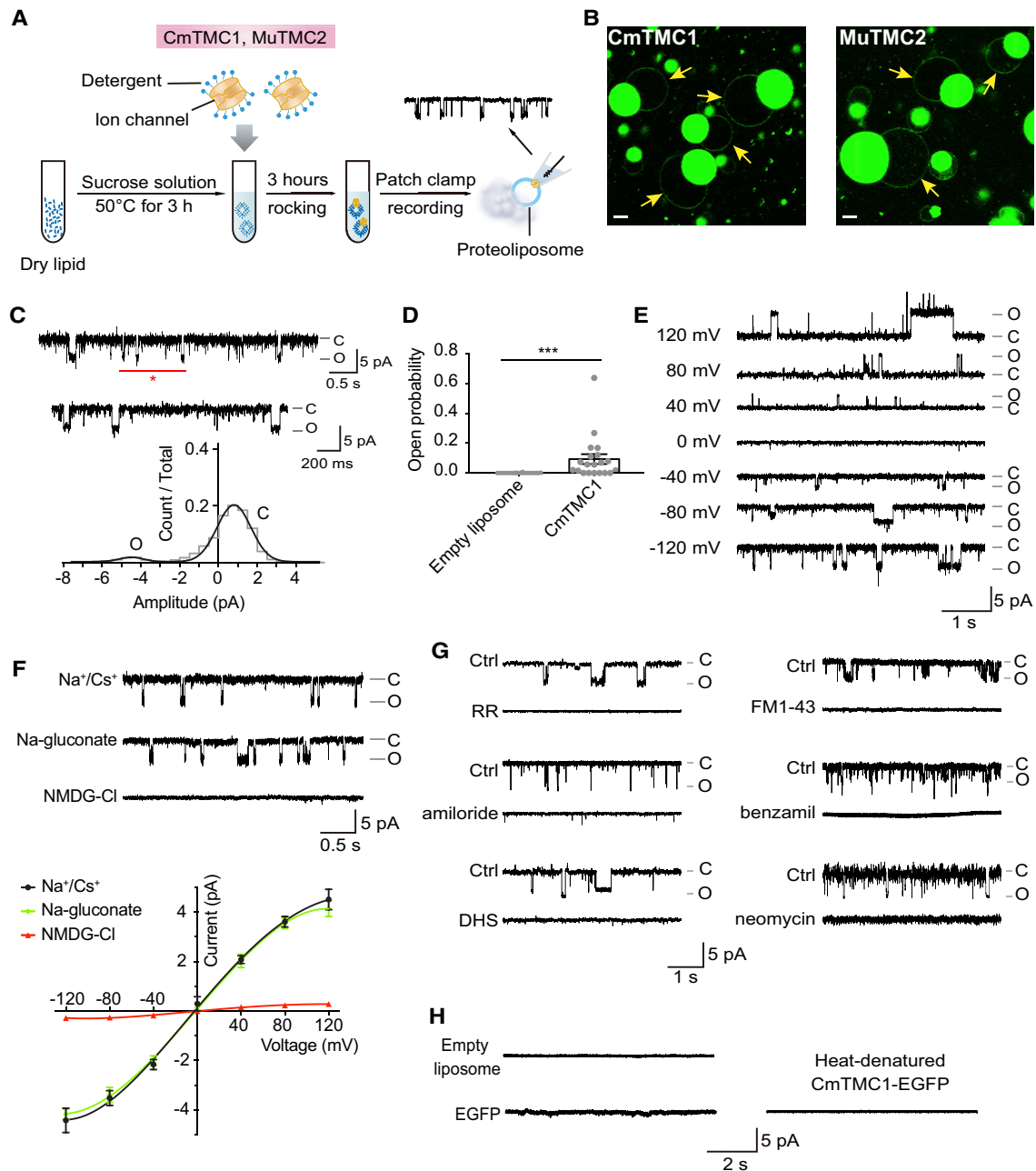


Figure 2. Spontaneous Channel Currents from Proteoliposomes Reconstituted with EGFP-Tagged CmTMC1

(A) Diagram showing the TMC proteoliposome reconstitution procedure with the sucrose method for patch-clamp recording. Liposomes are formed by adding sucrose solution to tubes with dry lipid; the purified proteins are then added and incorporated into the liposomes. A gigaohm seal is formed by application of suction, and the channel activity is then recorded.

(B) Representative images showing EGFP-labeled CmTMC1 (left) and MuTMC2 (right) incorporated into liposome membranes. The yellow arrows indicate membranes with EGFP-labeled CmTMC1 or MuTMC2. Scale bar, 10 μm .

(C) Representative spontaneous single-channel currents of CmTMC1 at -120 mV. The segment indicated by the red asterisk is enlarged and displayed in the lower trace. The normalized all-point amplitude histogram analysis of EGFP-tagged CmTMC1 with open (O) and closed (C) states at -120 mV is shown below. The distribution data were fitted by a sum of two Gaussians, and the peaks correspond to the C and O states.

(D) Scatterplots of the single-channel open probability (NPO) of CmTMC1. $n = 20$ each for empty liposomes and CmTMC1. In the 20 recordings for CmTMC1, 12 of them were detected with channel activities, 8 of them were not, and all 20 recording traces were utilized for calculation of the open probabilities. Error bars indicate the mean \pm SEM. Students' t test, $***p < 0.001$.

(E) Spontaneous currents recorded from the same patch of a proteoliposome reconstituted with CmTMC1 with voltage steps from -120 mV to $+120$ mV.

(legend continued on next page)

We then purified CmTMC1 and MuTMC2 proteins (Figure 1C). Mass spectrometry of the purified protein solutions verified that no endogenous ion channel protein from Sf9 cells was included in the purified TMC samples (Tables S2 and S3). Overall, CmTMC1 and MuTMC2 were found to be suitable for functional studies of TMC proteins.

We used globular standards to calibrate the Superose 6 increase 10/300 GL (29-0915-96, GE Healthcare) column and also run the purified EGFP-tagged CmTMC1 and EGFP-tagged MuTMC2 (Figure S2). The elution position indicated that the apparent molecular size of the EGFP-tagged CmTMC1 and MuTMC2 in n-dodecyl-beta-D-maltopyranoside and cholesteryl hemisuccinate (DDM-CHS) micelle would be 378 kDa and 362 kDa, respectively. Considering the molecular size of the EGFP-tagged CmTMC1 (99.1 kDa) and MuTMC2 monomer (88.5 kDa) and DDM-CHS micelle (91 kDa), the gel filtration analysis suggested that CmTMC1/MuTMC2 might form a dimer rather than a monomer or tetramer.

CmTMC1 and MuTMC2 Proteins Are Pore-Forming Ion Channels

To determine whether CmTMC1 could form functional ion channels in liposomes, the purified EGFP-tagged CmTMC1 protein was reconstituted in liposomes (Figure 2A). Although TMC proteins expressed in cultured cells are not localized in the cell membrane (Beurg et al., 2015; Kawashima et al., 2011; Labay et al., 2010; Wang et al., 2016; Zhao et al., 2014), we found that the purified EGFP-tagged CmTMC1 and EGFP-tagged MuTMC2 proteins are incorporated into the lipid membrane after reconstitution (Figures 2B and S3). The incorporation enabled us to perform further functional assays. Patch-clamp recordings with excised patches at a holding potential of -120 mV demonstrated that the liposomes reconstituted with CmTMC1 displayed spontaneous single-channel openings (Figures 2C and 2D). The all-point histogram of single-channel opening events showed that the average single-channel CmTMC1 current was -4.46 ± 0.11 pA ($n = 7$) at -120 mV (Figure 2C). Notably, although we calculated the single-channel open probability, we cannot exclude the possibility that these recordings are of multiple channels with low open probability in a single patch. The application of a series of voltage steps (from -120 mV to $+120$ mV in 40-mV increments) resulted in apparent voltage-dependent spontaneous single-channel openings (Figures 2E and S4A). Linear regression of the current-voltage relationship found slope conductance values of 40.5 ± 2.2 pS ($n = 6$) for CmTMC1-associated spontaneous currents (Figure 2F). The CmTMC1-induced currents were nearly eliminated in N-methyl-D-glucamine chloride (NMDG-Cl) solution but remained normal in Na-gluconate solution, indicating that the CmTMC1-associated current is primarily carried by a cation channel

(Figure 2F). Importantly, these CmTMC1-associated currents were blocked by ruthenium red (RR), FM1-43, amiloride, benzamil, and the aminoglycoside channel blockers dihydrostreptomycin (DHS) and neomycin (Figure 2G).

To further verify the ion channel activity of CmTMC1, we measured the activities of empty liposomes as well as that of liposomes reconstituted with EGFP only, and no channel activity was detected (Figure 2H). Heat-denatured purified CmTMC1 that was reconstituted in liposomes under identical conditions also failed to exhibit ion channel activity (Figure 2H).

We then examined whether TMC2 possesses ion channel activity by using purified MuTMC2 proteins. The liposome-reconstituted EGFP-MuTMC2 showed spontaneous single-channel openings in excised patches held at -120 mV (Figures 3A and 3B), similar to the response observed with CmTMC1. The estimated single-channel current of MuTMC2 was -3.81 ± 0.13 pA ($n = 7$) at -120 mV in Na^+/Cs^+ solution (Figure 3A), which was smaller than that of CmTMC1, as shown in the normalized all-point histogram of single-channel opening events. Voltage-dependent spontaneous channel openings of MuTMC2 were detected at different holding potentials (Figures 3C, 3D, and S4B). The single-channel conductance of MuTMC2 was 35.5 ± 2.2 pS ($n = 6$). Similar to the CmTMC1-associated current, the MuTMC2-associated current was absent in NMDG-Cl solution but remained normal in Na-gluconate solution, indicating that the MuTMC2-associated current was primarily carried by a cation channel (Figure 3D). We also measured the activity of heat-denatured purified MuTMC2 and found no channel activity (Figure 3E). Furthermore, the MuTMC2 current was also sensitive to RR, FM1-43, amiloride, benzamil, DHS, and neomycin (Figure 3F). Overall, our electrophysiological recordings with purified TMC proteins demonstrated that both CmTMC1 and MuTMC2 are pore-forming ion channels.

CmTMC1 and MuTMC2 Ion Channels Are Mechanosensitive

To examine whether reconstituted TMC proteins are directly gated by mechanical stimuli, we applied negative pressure through the patch-clamp recording pipette with a high-speed pressure clamp (HSPC) to stretch the membrane. First we determined whether we could successfully record pressure-activated current from liposomes reconstituted with the bacterial mechanosensitive ion channel *Escherichia coli* MscL (Häse et al., 1995). We observed pressure-induced MscL channel activity in excised patches (Figure S5). The pressure-activated MscL single-channel current was consistent with the previously reported value (Kloda and Martinac, 2002). Notably, we found a CmTMC1 channel current upon pressure application in patches held at -120 mV (Figure 4A). The single-channel open probability of CmTMC1 also increased upon pressure application

(F) Representative single-channel current traces recorded at -120 mV and current-voltage relationships of spontaneous currents recorded from EGFP-tagged CmTMC1 proteoliposomes. CmTMC1-induced currents were recorded in Na^+/Cs^+ , Na-gluconate, and NMDG-Cl solution. Data were fitted by a polynomial. $n = 6$. All error bars indicate the \pm SEM.

(G) The CmTMC1-associated currents were sensitive to channel blockers. The blockers were added to the bath solution, and recordings were then obtained from the same patch as the control. Each blocker was tested in an individual patch. The concentrations of the channel blockers were as follows: RR, 40 μM ; FM1-43, 3 μM ; amiloride, 0.2 mM; benzamil, 10 μM ; dihydrostreptomycin (DHS), 0.2 mM; neomycin, 1 mM.

(H) Liposomes that were empty, reconstituted with EGFP, and reconstituted with heat-denatured EGFP-tagged CmTMC1 failed to produce channel activity.

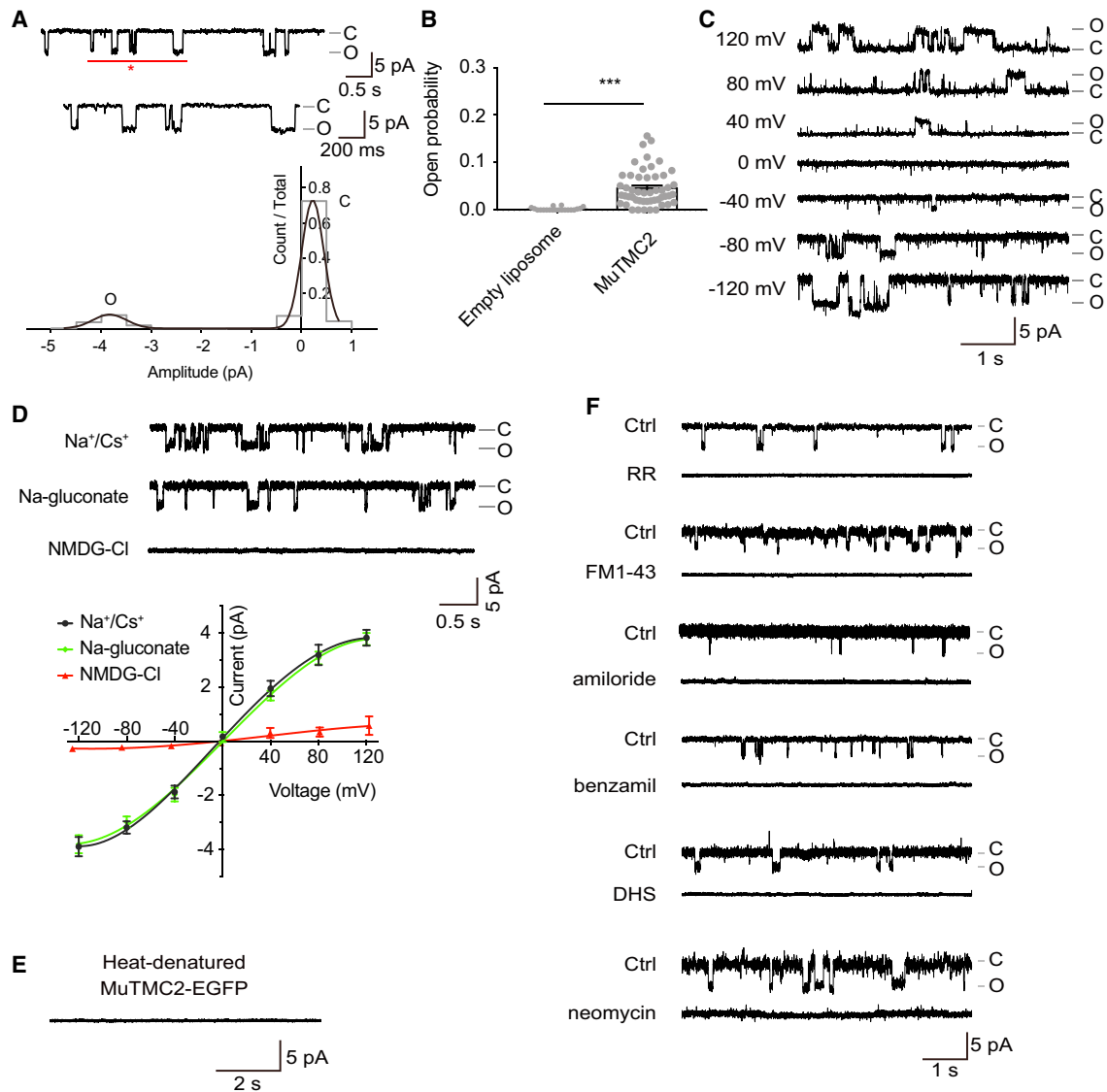


Figure 3. Spontaneous Channel Currents from Proteoliposomes Reconstituted with EGFP-Tagged MuTMC2

(A) Representative spontaneous single-channel currents of MuTMC2 at -120 mV. The segment indicated by the red asterisk is enlarged and displayed in a bottom trace. Normalized all-point amplitude histogram analysis of MuTMC2 with O and C states at -120 mV is shown below. The distribution data were fitted by a sum of two Gaussians, and the peaks correspond to the C and O states.

(B) Scatterplots of single-channel open probability (NPs) of MuTMC2. $n = 20$ for empty liposomes and $n = 50$ for MuTMC2, respectively. In the 50 recordings for MuTMC2, 45 of them were detected with channel activities, 5 of them were not, and all 50 recording traces were utilized for calculation of the open probabilities. Error bars represent the mean \pm SEM. Students' *t* test, $***p < 0.001$.

(C) Spontaneous single-channel currents recorded from the same patch of proteoliposome reconstituted with MuTMC2 with voltage steps from -120 mV to $+120$ mV.

(D) Representative single-channel current traces recorded at -120 mV and the current-voltage relationships of spontaneous currents recorded from proteoliposomes reconstituted with MuTMC2. MuTMC2-induced currents were recorded in Na^+/Cs^+ , Na-gluconate, and NMDG-Cl solutions. Data were fit by a polynomial. $n = 6$. All error bars indicate the \pm SEM.

(E) Heat-denatured EGFP-tagged MuTMC2 failed to produce channel activity.

(F) The MuTMC2-associated currents were sensitive to channel blockers.

(Figures S6A and S6C). As the pressure was gradually increased, the currents increased progressively (Figures 4B, 4C, and S7A). By resolving the single-channel current amplitudes of CmTMC1 (Figures 4E and 4F), we found that the single-channel current amplitude of channels activated by pres-

sure stimulation is the same as that for the spontaneously active channels (Figure 4G).

We also examined the empty and EGFP-reconstituted liposomes, and no pressure-induced activity was observed (Figures 4D and 4H). Furthermore, liposomes reconstituted with heat-

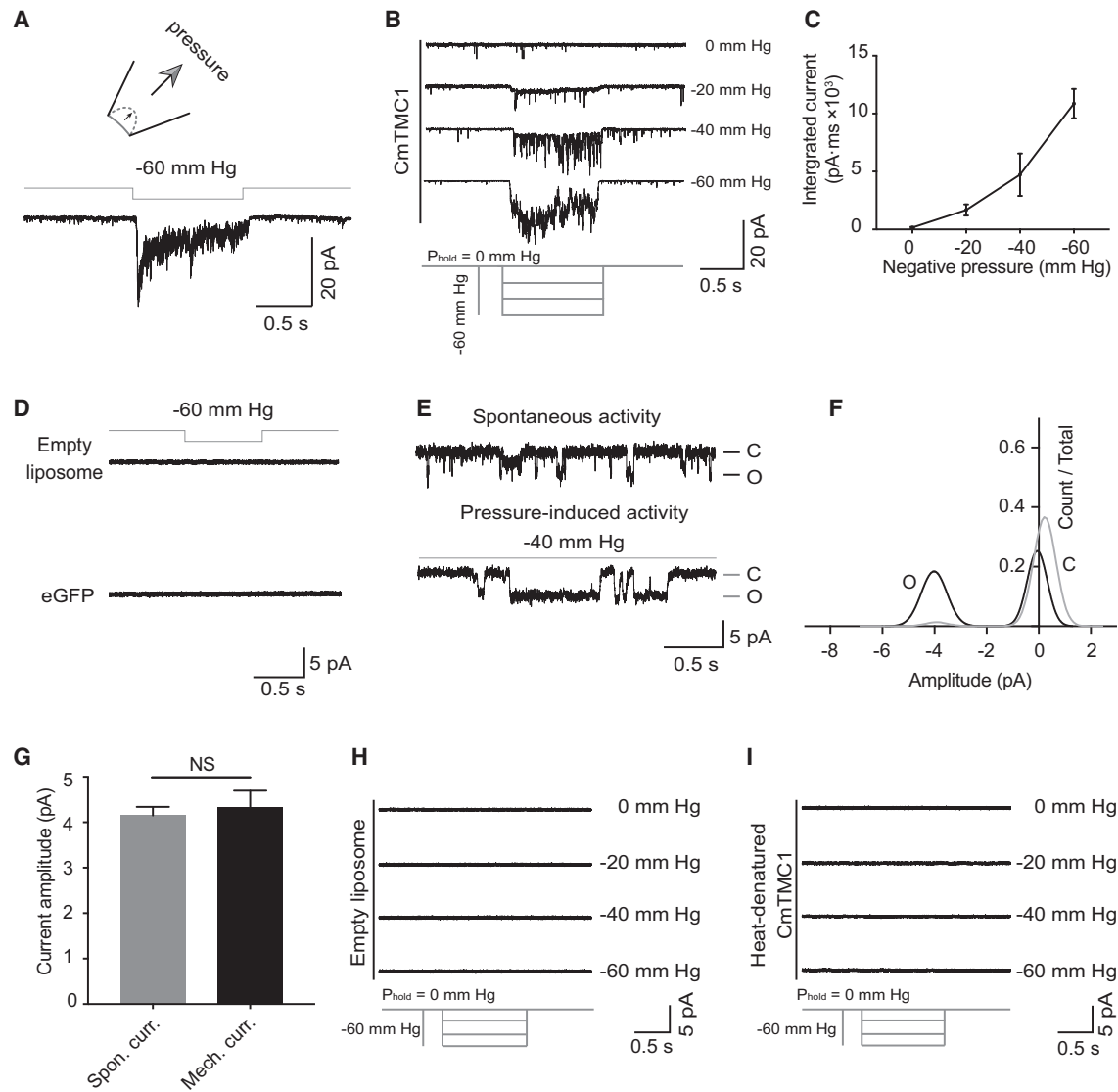


Figure 4. Proteoliposomes Reconstituted with CmTMC1 Exhibit Pressure-Activated Currents

(A) Top: schematic depicting a liposome membrane patch in a patch pipette to show the curvature change in the absence (solid line) and presence (dotted line) of negative pressure (arrow). Bottom: liposomes reconstituted with EGFP-tagged CmTMC1 showed mechanosensitive currents in response to negative pressure (–60 mm Hg) at –120 mV.

(B) Current responses to negative pressure applied to the same excised patch from a proteoliposome reconstituted with EGFP-tagged CmTMC1. Holding pressure (P_{hold}) = 0 mm Hg; 0 to –60 mm Hg, Δ Pressure = 20 mm Hg; holding potential = –120 mV.

(C) Pressure-dependent curve of the CmTMC1-associated currents. The area under the curve indicates the integrated current. $n = 6$. All error bars denote the mean \pm SEM.

(D) Empty liposomes and liposomes reconstituted with EGFP showed no channel activity with pressure stimulation.

(E) Representative single-channel activity (at –120 mV) from spontaneous EGFP-tagged CmTMC1 channels (top trace) and channels activated by mechanical stimulation via negative pressure on an excised patch (bottom trace).

(F) Histogram showing the increase in channel open probability after pressure stimulation. The black line denotes pressure-induced channel activity, and the gray line denotes spontaneous channel activity.

(G) Comparison of the single-channel current amplitude of spontaneously active channels and pressure-induced channels in an excised patch from the same liposome reconstituted with EGFP-tagged CmTMC1 at –120 mV. Spon. curr., spontaneous current; Mech. curr., mechanosensitive current. $n = 6$; paired t test; NS denotes statistically not significant ($p > 0.05$), error bars denote the mean \pm SEM.

(H) Empty liposomes displayed no mechanosensitive current in response to negative pressure.

(I) Heat-denatured EGFP-tagged CmTMC1 displayed no mechanosensitive current in response to negative pressure.

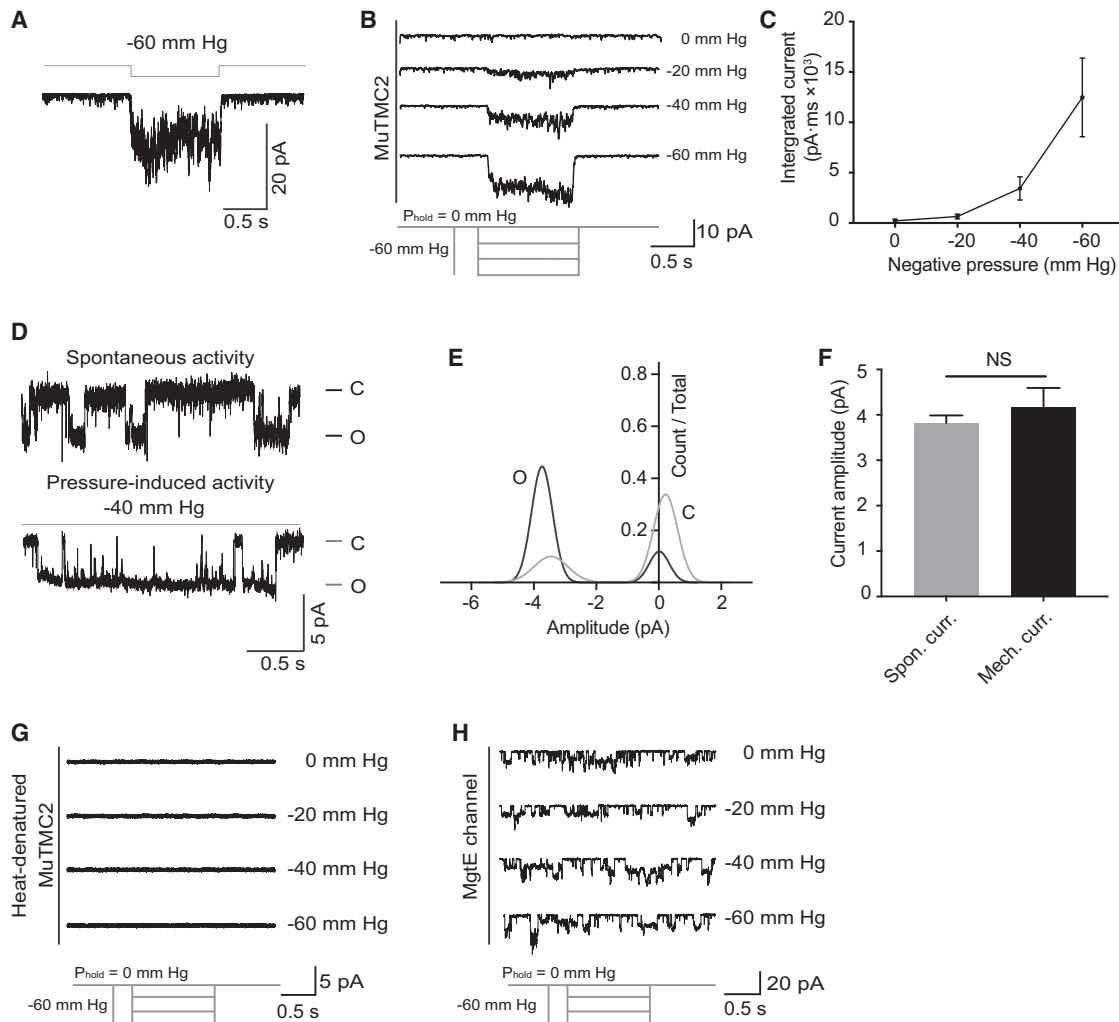


Figure 5. Proteoliposomes Reconstituted with MuTMC2 Exhibit Pressure-Activated Currents

(A) Liposomes reconstituted with EGFP-tagged MuTMC2 showed mechanosensitive currents in response to negative pressure. Holding potential = -120 mV. (B) Representative current responses to negative pressure applied to the same excised patch of a proteoliposome reconstituted with EGFP-tagged MuTMC2. (C) Pressure-dependent curve of the MuTMC2-associated currents. The area under the curve indicates the integrated current. $n = 6$. All error bars denote the mean \pm SEM.

(D) Representative single-channel activity at -120 mV of the spontaneously active MuTMC2 channel (top trace) and the channel activated by mechanical stimulation via negative pressure on an excised patch (bottom trace).

(E) Histogram showing the increase in channel open probability after pressure stimulation. The black line denotes pressure-induced channel activity, and the gray line denotes spontaneous channel activity.

(F) Comparison of the single-channel current amplitude of spontaneously active channels and pressure-induced channels in an excised patch from the same liposome reconstituted with MuTMC2 at -120 mV. Spon. curr., spontaneous current; Mech. curr., mechanosensitive current; $n = 6$; paired t test; NS denotes statistically not significant ($p > 0.05$), error bars denote the mean \pm SEM.

(G) Heat-denatured EGFP-tagged MuTMC2 displayed no mechanosensitive current in response to negative pressure.

(H) Proteoliposomes reconstituted with the MgtE channel showed no mechanosensitivity in response to negative pressure.

denatured CmTMC1 also exhibited no mechanically gated channel activity (Figure 4I).

MuTMC2 was also found to be a mechanically gated channel (Figure 5A), showing a progressive increase in current with increasing pressure stimulation at -120 mV (Figures 5B, 5C, and S7B). The single-channel open probability of MuTMC2 also increased upon pressure application (Figures S6B and S6D). By resolving the single-channel current amplitudes of

MuTMC2 (Figures 5D and 5E), we found that the single-channel current amplitude for channels activated by pressure stimulation was the same as that for the spontaneously active channels (Figure 5F). In contrast, we found that the mechanosensitivity disappeared in heat-denatured MuTMC2 (Figure 5G). Taken together, these results showed that CmTMC1 and MuTMC2 ion channels can be activated by mechanical force.

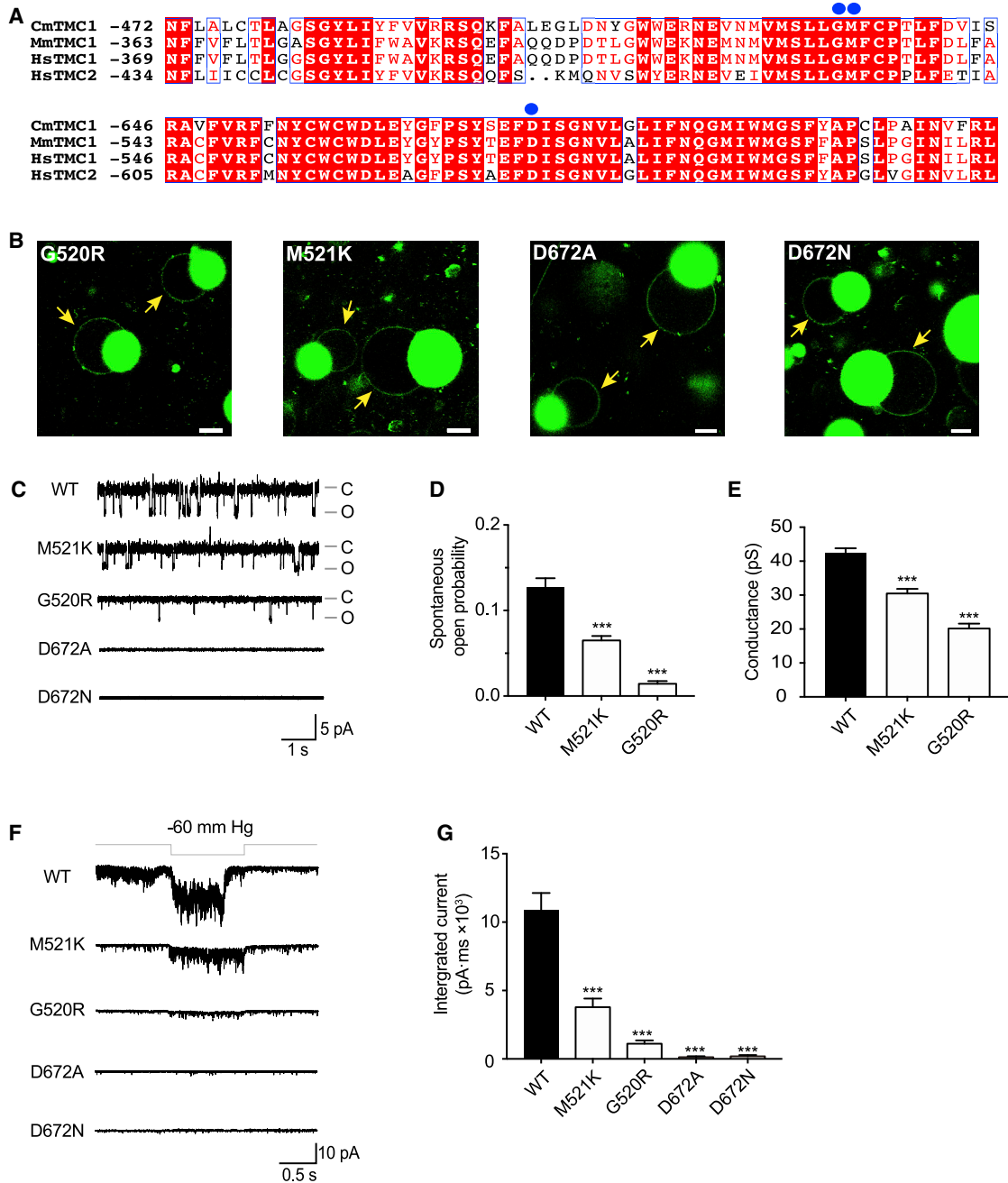


Figure 6. Deafness-Related CmTMC1 Mutants Exhibit No or Reduced Channel Activities

(A) Amino acid sequence alignment of the region close to Gly520, Met521, and Asp672 in the TMC proteins from *Chelonia mydas* (CmTMC1: XP_007065675.1), *Mus musculus* (MmTMC1: NP_083229.1), and *Homo sapiens* (HsTMC1: NP_619636.2, HsTMC2: NP_542789.2). The blue dots indicate Gly520, Met521, and Asp672 of CmTMC1. Strictly conserved and similar residues are highlighted with a red box and by a red letter, respectively. The sequence alignment figure was generated by ESPrnt 3.0 and Clustal Omega.

(B) Representative images showing EGFP-labeled CmTMC1 mutants (G520R, M521K, D672A, and D672N) incorporated into liposome membranes. The yellow arrows indicate membranes with EGFP-labeled CmTMC1 or MuTMC2. Scale bars, 10 μ m.

(C) Representative spontaneous single-channel current traces of WT CmTMC1 and CmTMC1 mutants (G520R, M521K, D672A, and D672N) at -120 mV.

(D) Single-channel open probabilities of WT CmTMC1 and the indicated CmTMC1 mutants under the spontaneous condition at -120 mV. $n = 10$, all of them have channel activities; unpaired t test, *** $p < 0.001$. All error bars denote the \pm SEM.

(E) The M521K and G520R mutations in CmTMC1 altered the single-channel conductance of the spontaneous current determined at -120 mV. $n = 10$. *** $p < 0.001$, unpaired t test. All error bars denote the mean \pm SEM.

(legend continued on next page)

To further validate our system, we examined the activity of another ion channel, MgtE, which has been reported to be a Mg^{2+} -selective ion channel (Hattori et al., 2009; Tomita et al., 2017), serving as a negative control. The single-channel conductance of MgtE spontaneous current at -120 mV was approximately 135.1 ± 12.22 pS ($n = 10$), which is consistent with previously reported results (Hattori et al., 2009). Indeed, although the reconstituted MgtE exhibited robust spontaneous channel activity, the channel was not activated by pressure application (Figure 5H).

Deafness-Related CmTMC1 Mutants Exhibit Reduced or No Ion Channel Activity

To examine the functional relationship between TMC channel function and hearing loss, we generated four CmTMC1 mutants: M521K, which corresponds to a semidominant *Tmc1* point mutation in the mouse, known as Beethoven (*Bth*) (Vreugde et al., 2002); D672N, corresponding to deafness (*dn*) (Kurima et al., 2002); D672A, in which the Asn was used in place of the Ala in the D672N mutant; and G520R, a mutant adjacent to the *Bth* mouse mutant (Yang et al., 2010). These sites—G520, M521, and D672—are highly conserved among TMC family proteins (Figures 6A and S1A). The four CmTMC1 mutants were purified with the same purification protocol as for wild-type (WT) CmTMC1, and purified EGFP-tagged CmTMC1 mutants were reconstituted into liposomes. The purified EGFP-tagged CmTMC1 mutants were well incorporated into the lipid membrane after reconstitution (Figure 6B). We found that the four CmTMC1 mutants all had detectable effects on either spontaneous activity or pressure-activated activity. Specifically, the single-channel open probabilities and single-channel conductance at -120 mV were reduced in the M521K and G520R mutants, whereas no channel activity was detected in the D672N and D672A mutants (Figures 6C–6E). Additionally, the M521K and G520R mutants showed a reduction in current response to negative pressure relative to the WT, and the D672N and D672A mutants had nearly no response to negative pressure (Figures 6F and 6G). However, we cannot exclude the possibility that these recordings are of multiple channels with low open probability in a single patch, and we are not sure how many channels are associated with the integrated currents. Figure 6G depends on N being the same under all conditions. These results further support that the purified CmTMC1, not endogenous proteins from Sf9 cells, exhibited ion channel activity. These data also indicate a functional correlation between the channel function of TMC1 and hearing.

DISCUSSION

For a protein to be considered as the mechanotransduction ion channel for hearing, it should meet certain criteria (Arnadóttir and Chalfie, 2010; Christensen and Corey, 2007; Ranade et al., 2015). First, the protein should be localized in the stereocilia tips of hair cells and required for mechanotransduction in hair

cells, and further, the protein should be a pore-forming mechanosensitive ion channel. TMC1 and TMC2 are necessary for the mechanotransduction currents of hair cells in mice, and TMC1 mutations cause hearing loss in humans (Kawashima et al., 2011; Kurima et al., 2002; Marcotti et al., 2006; Pan et al., 2013; Vreugde et al., 2002). Although TMC1 and TMC2 double knockout mice still have “reverse polarity” currents, this current is abolished in *Piezo2* knockout mice, and *Piezo2* knockout mice have no hearing defect (Qiu and Müller, 2018; Wu et al., 2017), demonstrating that the reverse polarity currents are not generated by the auditory transduction channel. Both mouse TMC1 and TMC2 are expressed in hair cells and localize in stereocilia tips, where mechanotransduction occurs (Beurg et al., 2015; Kawashima et al., 2015; Kurima et al., 2015). TMC1 and TMC2 are both capable of restoring auditory function in TMC1 mutant mice, indicating a highly similar role of TMC1 and TMC2 in hearing transduction (Askew et al., 2015). A recent study showed that TMC1 is a dimer and that point mutations can alter the permeation properties of mechanosensory transduction (Pan et al., 2018). Here, our study showed that purified CmTMC1 and MuTMC2 proteins are pore-forming ion channels and can respond to mechanical stimuli; the purified CmTMC1 and MuTMC2 proteins reconstituted in liposomes show robust channel activity and are activated by a mechanical stimulus. Although the current study focuses primarily on CmTMC1 and MuTMC2, the strong evolutionary conservation of CmTMC1 and MuTMC2 with human TMC1 and TMC2 (Figure S1) suggests that mammalian TMC1 and TMC2 are also likely to be ion channels and to be mechanosensitive. Taken together with the results of previous studies (Askew et al., 2015; Beurg et al., 2015; Kawashima et al., 2011; Kurima et al., 2002, 2015; Marcotti et al., 2006; Pan et al., 2013, 2018), our results suggest that TMC1 and TMC2 can form mechano-gated channels in vertebrates that meet most of the criteria that have been proposed, strongly supporting the link between auditory transduction and TMC1/2.

There is a gradient increase in the single-channel conductance of the mechanosensitive channels in turtle hair cells, raising the possibility that the native auditory transduction channel consists of several different subunits (Ricci et al., 2003). A recent study (Beurg et al., 2018) suggested that there might be multiple levels of opening for transduction channels. This study also indicated that the conductance of mouse TMC1 is approximately 70 pS and that the conductance of mouse TMC2 is approximately 50 pS. The single-channel conductance of the mouse mechanotransduction channel in this study (Beurg et al., 2018) is consistent with our single-channel conductance for CmTMC1 (40.5 ± 2.2 pS) and MuTMC2 (35.5 ± 2.2 pS). A classic study by Holton and Hudspeth (1986) suggested that the single-channel conductance of the transduction channel of hair cells in bullfrogs is approximately 17 pS at room temperature. Additionally, CmTMC1 and MuTMC2 are from different species (turtle and budgerigar) than mouse and it is possible that CmTMC1 and MuTMC2 have a different single-channel conductance than the mouse TMC1 and TMC2 proteins.

(F) Representative pressure-induced current traces of WT CmTMC1 and its mutants (G520R, M521K, D672A, and D672N) at -120 mV.

(G) Comparison of the pressure-induced currents of WT CmTMC1 and its mutants (G520R, M521K, D672A, and D672N) at -120 mV. $n = 6$. Unpaired *t* test, *** $p < 0.001$. All error bars represent the mean \pm SEM.

Although our study suggests that TMC1 and TMC2 proteins are pore-forming subunits of the auditory transduction channel, it is also possible that TMHS/LHFPL5 and TMIE are integral components of the native auditory transduction channel (Gleason et al., 2009; Longo-Guess et al., 2007; Mitchem et al., 2002; Naz et al., 2002; Shabbir et al., 2006; Xiong et al., 2012; Zhao et al., 2014). Calcium and integrin-binding protein 2 (CIB2), cadherin 23 (CDH23), and protocadherin 15 (PCDH15) have been shown to directly or indirectly interact with TMC proteins for the gating or modulation of TMC function (Giese et al., 2017; Kazmierczak et al., 2007; Maeda et al., 2014; Riazuddin et al., 2012). PIP2 can regulate the pore properties and adaptation of the auditory mechanotransduction channel (Effertz et al., 2017). Specifically, Maeda et al. (2014) showed a direct interaction between PCDH15 and TMC proteins, which is required for hair cell mechanosensitivity. Additionally, the authors found that TMCs interact with PCDH15 through the very N-terminal domain. It is possible that the N terminus of TMC may interact with PCDH15 to maintain the closed state of the channel in the absence of external force. In the current study, we truncated the N termini of TMC1 and TMC2, and these truncations might help the TMC1 and TMC2 show the spontaneous activity without external force.

How these proteins and molecules coordinate to gate the auditory transduction channels and modulate the channel properties remains unclear. Our results suggest that TMC1 and TMC2 are the pore-forming subunits of the auditory transduction channel and lay the foundation for further studies.

STAR★METHODS

Detailed methods are provided in the online version of this paper and include the following:

- KEY RESOURCE TABLE
- LEAD CONTACT AND MATERIALS AVAILABILITY
- EXPERIMENTAL MODEL AND SUBJECT DETAILS
- METHOD DETAILS
 - Fluorescence-detection size-exclusion chromatography (FSEC)
 - Protein expression and purification
 - Mass spectrometry
 - Reconstitution of target proteins in liposomes
 - Patch-clamp recording
- QUANTIFICATION AND STATISTICAL ANALYSIS
- DATA AND CODE AVAILABILITY

SUPPLEMENTAL INFORMATION

Supplemental Information can be found online at <https://doi.org/10.1016/j.neuron.2019.10.017>.

ACKNOWLEDGMENTS

We thank all Yan laboratory members for support. The research was supported by funds from the National Key R&D Program of China Project (2017YFA0103900 to Z.Y.); the National Natural Science Foundation of China (31571083 and 31970931 to Z.Y.); the Program for Professor of Special Appointment (Eastern Scholar of Shanghai, TP2014008 to Z.Y.); the Shanghai Rising-Star Program (14QA1400800 to Z.Y.); the National Key R&D Program of

China (2016YFA0502800 to M.H. and Z.Y.); and the National Natural Science Foundation of China (31570838 and 31650110469 to M.H.). Additional support was provided by grants from the Thousand Talent Program for Young Outstanding Scientists of China (to Z.Y. and M.H.). This work was also supported in part by the Research Funds for Graduate Students of Fudan University (to Y.J.) and the International Postdoctoral Exchange Fellowship Program from the Office of China Postdoctoral Council (to Y. Zhao.). The research was also supported by grants from the AMED-CREST Program “The Creation of Basic Medical Technologies to Clarify and Control the Mechanisms Underlying Chronic Inflammation” (to O.N.); grants from the Platform for Drug Discovery, Informatics and Structural Life Science from the Ministry of Education, Culture, Sports, Science and Technology (MEXT) (to O.N.); and grants from JSPS KAKENHI (16H06294 and 24227004 to O.N.).

AUTHOR CONTRIBUTIONS

Z.Y. conceived the project and designed the experiments. O.N., M.H., and Z.Y. supervised the project and provided guidance throughout. Y.J. performed the liposome patch-clamp recording experiments with the assistance of C.P. Y.J. performed the confocal images with the assistance of Y. Zhang. Y. Zhao conducted the expression screening of TMC proteins and purified TMC proteins with the assistance of Y.W. T.K. contributed to the purification of TMC2 protein. Y.J., Y. Zhao, M.H., and Z.Y. wrote the manuscript. All authors discussed the results and commented on the manuscript.

DECLARATION OF INTERESTS

The authors declare no competing interests.

Received: June 7, 2018

Revised: September 5, 2019

Accepted: October 9, 2019

Published: November 21, 2019

REFERENCES

- Arnadóttir, J., and Chalfie, M. (2010). Eukaryotic mechanosensitive channels. *Annu. Rev. Biophys.* 39, 111–137.
- Askew, C., Rochat, C., Pan, B., Asai, Y., Ahmed, H., Child, E., Schneider, B.L., Aebischer, P., and Holt, J.R. (2015). *Tmc* gene therapy restores auditory function in deaf mice. *Sci. Transl. Med.* 7, 295ra108.
- Battle, A.R., Petrov, E., Pal, P., and Martinac, B. (2009). Rapid and improved reconstitution of bacterial mechanosensitive ion channel proteins MscS and MscL into liposomes using a modified sucrose method. *FEBS Lett.* 583, 407–412.
- Beurg, M., Xiong, W., Zhao, B., Müller, U., and Fettiplace, R. (2015). Subunit determination of the conductance of hair-cell mechanotransducer channels. *Proc. Natl. Acad. Sci. USA* 112, 1589–1594.
- Beurg, M., Cui, R., Goldring, A.C., Ebrahim, S., Fettiplace, R., and Kachar, B. (2018). Variable number of TMC1-dependent mechanotransducer channels underlie tonotopic conductance gradients in the cochlea. *Nat. Commun.* 9, 2185.
- Chatzigeorgiou, M., Bang, S., Hwang, S.W., and Schafer, W.R. (2013). *tmc-1* encodes a sodium-sensitive channel required for salt chemosensation in *C. elegans*. *Nature* 494, 95–99.
- Christensen, A.P., and Corey, D.P. (2007). TRP channels in mechanosensation: direct or indirect activation? *Nat. Rev. Neurosci.* 8, 510–521.
- Coleman, J.A., Green, E.M., and Gouaux, E. (2016). X-ray structures and mechanism of the human serotonin transporter. *Nature* 532, 334–339.
- Corey, D.P., and Hudspeth, A.J. (1979). Ionic basis of the receptor potential in a vertebrate hair cell. *Nature* 281, 675–677.
- Crawford, A.C., Evans, M.G., and Fettiplace, R. (1991). The actions of calcium on the mechano-electrical transducer current of turtle hair cells. *J. Physiol.* 434, 369–398.

- Effertz, T., Becker, L., Peng, A.W., and Ricci, A.J. (2017). Phosphoinositol-4,5-bisphosphate regulates auditory hair-cell mechanotransduction-channel pore properties and fast adaptation. *J. Neurosci.* **37**, 11632–11646.
- Fettiplace, R. (2016). Is TMC1 the hair cell mechanotransducer channel? *Biophys. J.* **111**, 3–9.
- Giese, A.P.J., Tang, Y.Q., Sinha, G.P., Bowl, M.R., Goldring, A.C., Parker, A., Freeman, M.J., Brown, S.D.M., Riazuddin, S., Fettiplace, R., et al. (2017). CIB2 interacts with TMC1 and TMC2 and is essential for mechanotransduction in auditory hair cells. *Nat. Commun.* **8**, 43.
- Gillespie, P.G., and Müller, U. (2009). Mechanotransduction by hair cells: models, molecules, and mechanisms. *Cell* **139**, 33–44.
- Gleason, M.R., Nagiel, A., Jamet, S., Vologodskaja, M., López-Schier, H., and Hudspeth, A.J. (2009). The transmembrane inner ear (*Tmie*) protein is essential for normal hearing and balance in the zebrafish. *Proc. Natl. Acad. Sci. USA* **106**, 21347–21352.
- Guo, Y., Wang, Y., Zhang, W., Meltzer, S., Zanini, D., Yu, Y., Li, J., Cheng, T., Guo, Z., Wang, Q., et al. (2016). Transmembrane channel-like (*tmc*) gene regulates *Drosophila* larval locomotion. *Proc. Natl. Acad. Sci. USA* **113**, 7243–7248.
- Häse, C.C., Le Dain, A.C., and Martinac, B. (1995). Purification and functional reconstitution of the recombinant large mechanosensitive ion channel (*MscL*) of *Escherichia coli*. *J. Biol. Chem.* **270**, 18329–18334.
- Hattori, M., Iwase, N., Furuya, N., Tanaka, Y., Tsukazaki, T., Ishitani, R., Maguire, M.E., Ito, K., Maturana, A., and Nureki, O. (2009). Mg²⁺-dependent gating of bacterial MgtE channel underlies Mg²⁺ homeostasis. *EMBO J.* **28**, 3602–3612.
- Hattori, M., Hibbs, R.E., and Gouaux, E. (2012). A fluorescence-detection size-exclusion chromatography-based thermostability assay for membrane protein precrystallization screening. *Structure* **20**, 1293–1299.
- Hibbs, R.E., and Gouaux, E. (2011). Principles of activation and permeation in an anion-selective Cys-loop receptor. *Nature* **474**, 54–60.
- Holt, T., and Hudspeth, A.J. (1986). The transduction channel of hair cells from the bull-frog characterized by noise analysis. *J. Physiol.* **375**, 195–227.
- Hudspeth, A.J., and Corey, D.P. (1977). Sensitivity, polarity, and conductance change in the response of vertebrate hair cells to controlled mechanical stimuli. *Proc. Natl. Acad. Sci. USA* **74**, 2407–2411.
- Kawashima, Y., Géléoc, G.S., Kurima, K., Labay, V., Lelli, A., Asai, Y., Makishima, T., Wu, D.K., Della Santina, C.C., Holt, J.R., and Griffith, A.J. (2011). Mechanotransduction in mouse inner ear hair cells requires transmembrane channel-like genes. *J. Clin. Invest.* **121**, 4796–4809.
- Kawashima, Y., Kurima, K., Pan, B., Griffith, A.J., and Holt, J.R. (2015). Transmembrane channel-like (*TMC*) genes are required for auditory and vestibular mechanosensation. *Pflugers Arch.* **467**, 85–94.
- Kawate, T., and Gouaux, E. (2006). Fluorescence-detection size-exclusion chromatography for precrystallization screening of integral membrane proteins. *Structure* **14**, 673–681.
- Kawate, T., Michel, J.C., Birdsong, W.T., and Gouaux, E. (2009). Crystal structure of the ATP-gated P2X₄ ion channel in the closed state. *Nature* **460**, 592–598.
- Kazmierczak, P., Sakaguchi, H., Tokita, J., Wilson-Kubalek, E.M., Milligan, R.A., Müller, U., and Kachar, B. (2007). Cadherin 23 and protocadherin 15 interact to form tip-link filaments in sensory hair cells. *Nature* **449**, 87–91.
- Kloda, A., and Martinac, B. (2002). Common evolutionary origins of mechanosensitive ion channels in Archaea, Bacteria and cell-walled Eukarya. *Archaea* **1**, 35–44.
- Kurima, K., Peters, L.M., Yang, Y., Riazuddin, S., Ahmed, Z.M., Naz, S., Arnaud, D., Drury, S., Mo, J., Makishima, T., et al. (2002). Dominant and recessive deafness caused by mutations of a novel gene, *TMC1*, required for cochlear hair-cell function. *Nat. Genet.* **30**, 277–284.
- Kurima, K., Ebrahim, S., Pan, B., Sedlacek, M., Sengupta, P., Millis, B.A., Cui, R., Nakanishi, H., Fujikawa, T., Kawashima, Y., et al. (2015). TMC1 and TMC2 localize at the site of mechanotransduction in mammalian inner ear hair cell stereocilia. *Cell Rep.* **12**, 1606–1617.
- Labay, V., Weichert, R.M., Makishima, T., and Griffith, A.J. (2010). Topology of transmembrane channel-like gene 1 protein. *Biochemistry* **49**, 8592–8598.
- Lee, C.H., Lü, W., Michel, J.C., Goehring, A., Du, J., Song, X., and Gouaux, E. (2014). NMDA receptor structures reveal subunit arrangement and pore architecture. *Nature* **511**, 191–197.
- Longo-Guess, C.M., Gagnon, L.H., Fritsch, B., and Johnson, K.R. (2007). Targeted knockout and *lacZ* reporter expression of the mouse *Tmhs* deafness gene and characterization of the *hscy-2J* mutation. *Mamm. Genome* **18**, 646–656.
- Maeda, R., Kindt, K.S., Mo, W., Morgan, C.P., Erickson, T., Zhao, H., Clemens-Grisham, R., Barr-Gillespie, P.G., and Nicolson, T. (2014). Tip-link protein protocadherin 15 interacts with transmembrane channel-like proteins TMC1 and TMC2. *Proc. Natl. Acad. Sci. USA* **111**, 12907–12912.
- Manley, G.A., and Köppl, C. (2008). What have lizard ears taught us about auditory physiology? *Hear. Res.* **238**, 3–11.
- Marcotti, W., Erven, A., Johnson, S.L., Steel, K.P., and Kros, C.J. (2006). *Tmc1* is necessary for normal functional maturation and survival of inner and outer hair cells in the mouse cochlea. *J. Physiol.* **574**, 677–698.
- Martinac, B., Rohde, P.R., Battle, A.R., Petrov, E., Pal, P., Foo, A.F., Vásquez, V., Huynh, T., and Kloda, A. (2010). Studying mechanosensitive ion channels using liposomes. *Methods Mol. Biol.* **606**, 31–53.
- Mitchem, K.L., Hibbard, E., Beyer, L.A., Bosom, K., Dootz, G.A., Dolan, D.F., Johnson, K.R., Raphael, Y., and Kohrman, D.C. (2002). Mutation of the novel gene *Tmie* results in sensory cell defects in the inner ear of spinner, a mouse model of human hearing loss DFNB6. *Hum. Mol. Genet.* **11**, 1887–1898.
- Naz, S., Giguere, C.M., Kohrman, D.C., Mitchem, K.L., Riazuddin, S., Morell, R.J., Ramesh, A., Srisailpathy, S., Deshmukh, D., Riazuddin, S., et al. (2002). Mutations in a novel gene, *TMIE*, are associated with hearing loss linked to the *DFNB6* locus. *Am. J. Hum. Genet.* **71**, 632–636.
- Ohmori, H. (1985). Mechano-electrical transduction currents in isolated vestibular hair cells of the chick. *J. Physiol.* **359**, 189–217.
- Pan, B., Géléoc, G.S., Asai, Y., Horwitz, G.C., Kurima, K., Ishikawa, K., Kawashima, Y., Griffith, A.J., and Holt, J.R. (2013). TMC1 and TMC2 are components of the mechanotransduction channel in hair cells of the mammalian inner ear. *Neuron* **79**, 504–515.
- Pan, B., Akyuz, N., Liu, X.P., Asai, Y., Nist-Lund, C., Kurima, K., Derfler, B.H., Gyorgy, B., Limapichat, W., Walujkar, S., et al. (2018). TMC1 Forms the Pore of Mechanosensory Transduction Channels in Vertebrate Inner Ear Hair Cells. *Neuron* **99**, 736–753.e6.
- Penmatsa, A., Wang, K.H., and Gouaux, E. (2013). X-ray structure of dopamine transporter elucidates antidepressant mechanism. *Nature* **503**, 85–90.
- Pickles, J.O., Brix, J., Comis, S.D., Gleich, O., Köppl, C., Manley, G.A., and Osborne, M.P. (1989). The organization of tip links and stereocilia on hair cells of bird and lizard basilar papillae. *Hear. Res.* **41**, 31–41.
- Qiu, X., and Müller, U. (2018). Mechanically gated ion channels in mammalian hair cells. *Front. Cell. Neurosci.* **12**, 100.
- Ranade, S.S., Syeda, R., and Patapoutian, A. (2015). Mechanically Activated Ion Channels. *Neuron* **87**, 1162–1179.
- Riazuddin, S., Belyantseva, I.A., Giese, A.P., Lee, K., Indzhukulian, A.A., Nandamuri, S.P., Yousaf, R., Sinha, G.P., Lee, S., Terrell, D., et al. (2012). Alterations of the CIB2 calcium- and integrin-binding protein cause Usher syndrome type 1J and nonsyndromic deafness DFNB48. *Nat. Genet.* **44**, 1265–1271.
- Ricci, A.J., and Fettiplace, R. (1997). The effects of calcium buffering and cyclic AMP on mechano-electrical transduction in turtle auditory hair cells. *J. Physiol.* **501**, 111–124.
- Ricci, A.J., Crawford, A.C., and Fettiplace, R. (2003). Tonotopic variation in the conductance of the hair cell mechanotransducer channel. *Neuron* **40**, 983–990.
- Schwander, M., Kachar, B., and Müller, U. (2010). Review series: The cell biology of hearing. *J. Cell Biol.* **190**, 9–20.

- Shabbir, M.I., Ahmed, Z.M., Khan, S.Y., Riazuddin, S., Waryah, A.M., Khan, S.N., Camps, R.D., Ghosh, M., Kabra, M., Belyantseva, I.A., et al. (2006). Mutations of human *TMHS* cause recessively inherited non-syndromic hearing loss. *J. Med. Genet.* *43*, 634–640.
- Sobolevsky, A.I., Rosconi, M.P., and Gouaux, E. (2009). X-ray structure, symmetry and mechanism of an AMPA-subtype glutamate receptor. *Nature* *462*, 745–756.
- Tomita, A., Zhang, M., Jin, F., Zhuang, W., Takeda, H., Maruyama, T., Osawa, M., Hashimoto, K.I., Kawasaki, H., Ito, K., et al. (2017). ATP-dependent modulation of MgtE in Mg^{2+} homeostasis. *Nat. Commun.* *8*, 148.
- Tsirigos, K.D., Peters, C., Shu, N., Käll, L., and Elofsson, A. (2015). The TOPCONS web server for consensus prediction of membrane protein topology and signal peptides. *Nucleic Acids Res.* *43* (W1), W401–7.
- Tsuprun, V., Goodyear, R.J., and Richardson, G.P. (2004). The structure of tip links and kinociliary links in avian sensory hair bundles. *Biophys. J.* *87*, 4106–4112.
- Vreugde, S., Erven, A., Kros, C.J., Marcotti, W., Fuchs, H., Kurima, K., Wilcox, E.R., Friedman, T.B., Griffith, A.J., Balling, R., et al. (2002). Beethoven, a mouse model for dominant, progressive hearing loss DFNA36. *Nat. Genet.* *30*, 257–258.
- Wang, X., Li, G., Liu, J., Liu, J., and Xu, X.Z. (2016). TMC-1 mediates alkaline sensation in *C. elegans* through nociceptive neurons. *Neuron* *91*, 146–154.
- Wu, Z., Grillet, N., Zhao, B., Cunningham, C., Harkins-Perry, S., Coste, B., Ranade, S., Zebajadi, N., Beurg, M., Fettiplace, R., et al. (2017). Mechanosensory hair cells express two molecularly distinct mechanotransduction channels. *Nat. Neurosci.* *20*, 24–33.
- Xiong, W., Grillet, N., Elledge, H.M., Wagner, T.F., Zhao, B., Johnson, K.R., Kazmierczak, P., and Müller, U. (2012). TMHS is an integral component of the mechanotransduction machinery of cochlear hair cells. *Cell* *151*, 1283–1295.
- Yang, T., Kahrizi, K., Bazazzadegan, N., Meyer, N., Najmabadi, H., and Smith, R.J. (2010). A novel mutation adjacent to the *Bth* mouse mutation in the *TMC1* gene makes this mouse an excellent model of human deafness at the DFNA36 locus. *Clin. Genet.* *77*, 395–398.
- Yue, X., Zhao, J., Li, X., Fan, Y., Duan, D., Zhang, X., Zou, W., Sheng, Y., Zhang, T., Yang, Q., et al. (2018). TMC proteins modulate egg laying and membrane excitability through a background leak conductance in *C. elegans*. *Neuron* *97*, 571–585.e5.
- Zhao, B., Wu, Z., Grillet, N., Yan, L., Xiong, W., Harkins-Perry, S., and Müller, U. (2014). TMIE is an essential component of the mechanotransduction machinery of cochlear hair cells. *Neuron* *84*, 954–967.

STAR★METHODS

KEY RESOURCE TABLE

REAGENT or RESOURCE	SOURCE	IDENTIFIER
Bacterial and Virus Strains		
<i>Escherichia coli</i> : DH10 Bac strain	GIBCO	Cat#:10361012
Chemicals, Peptides, and Recombinant Proteins		
Ni-NTA agarose beads	QIAGEN	1018236
DDM	Anatrace	69227-93-6
CHS	Sigma-Aldrich	C6512-25G
FuGENE HD Transfection Reagent	Promega	E2311
SIM SF	Sino Biological	MSF1
Salts, acids, bases for recording solutions	Sigma-Aldrich	Stock
FM1-43	Thermo Fisher	T3163
Dihydrostreptomycin	Sigma-Aldrich	D7253
Amiloride	Sigma-Aldrich	A4562
Benzamil	Sigma-Aldrich	B2417
Neomycin	Sigma-Aldrich	N6386
Ruthenium red	Sigma-Aldrich	R2751
Deposited Data		
Raw and analyzed data	This study; Mendelay data	https://doi.org/10.17632/mcswckj5wd.1
Experimental Models: Cell Lines		
<i>Spodoptera frugiperda</i> ovary: Sf9 cells	GIBCO	Cat#:11496015; RRID: CVCL_0549
Recombinant DNA		
CmTMC1 (XP_007065675.1) in pFastBac	This study	N/A
MuTMC2 (XP_012985179.1) in pFastBac	This study	N/A
EGFP in pFastBac	This study	N/A
CmTMC1 (XP_007065675.1, G520R) in pFastBac	This study	N/A
CmTMC1 (XP_007065675.1, M521K) in pFastBac	This study	N/A
CmTMC1 (XP_007065675.1, D672N) in pFastBac	This study	N/A
CmTMC1 (XP_007065675.1, D672A) in pFastBac	This study	N/A
Software and Algorithms		
PClamp 10 software suite	Molecular Devices	https://www.moleculardevices.com/products/axon-patch-clamp-system
GraphPad Prism 7	GraphPad Software	https://www.graphpad.com/scientific-software/prism/
Clustal Omega sequence alignment software	European Bioinformatics Institute	https://www.ebi.ac.uk/Tools/msa/clustalo/
Other		
Borosilicate thick wall glass 1.5 OD/0.86 ID	Sutter Instrument	BF150-86-10

LEAD CONTACT AND MATERIALS AVAILABILITY

All unique/stable reagents generated in this study are available from the Lead Contact with a completed Materials Transfer Agreement. Further requests for information and for resources and reagents should be directed to and will be fulfilled by the Lead Contact, Zhiqiang Yan (zqyan@fudan.edu.cn).

EXPERIMENTAL MODEL AND SUBJECT DETAILS

Spodoptera frugiperda (Sf9) insect cells were cultivated in suspension culture at 27°C in Serum Free, SIM SF medium (Sino Biological) and routinely passaged every third day. These cells are from a commercially available cell line and are authenticated by the manufacturer. Sex: female.

METHOD DETAILS

Fluorescence-detection size-exclusion chromatography (FSEC)

Orthologs for TMC1 and TMC2 were cloned into the pFastBac vector with an octahistidine tag and EGFP at its N terminus. Sf9 cells (GIBCO) transfected using FuGENE HD (Promega) were harvested and solubilized in TBS (20 mM Tris pH 8.0, and 150 mM NaCl), 2% n-dodecyl-beta-D-maltopyranoside (DDM), and 0.4% cholesteryl hemisuccinate (CHS) for 1 hour at 4°C and then centrifuged at 25,000 rpm for 20 minutes to remove unsolubilized cells. Supernatants were injected onto a Superdex® 200 increase 10/300 column (28-9909-44, GE Healthcare), pre-equilibrated with TBS, 0.05% DDM and 0.01% CHS and detected by a fluorescence detector (excitation: 488 nm and emission: 520 nm for the GFP signal).

Protein expression and purification

CmTMC1 (XP_007065675.1, residue 244-842) and MuTMC2 (XP_012985179.1, residue 180-690) genes were synthesized and subcloned into the pFastBac vector with an N-terminal octahistidine tag and EGFP. The N-terminal and C-terminal truncations of CmTMC1 and MuTMC2 did not include the transmembrane domains of CmTMC1 (residue 297-818) and MuTMC2 (residue 229-689) predicted by the TOPCONS server (Tsirigos et al., 2015). These truncations were introduced to increase the expression and stability of the TMC proteins for purification.

TMC proteins used for reconstitution were expressed in Sf9 cells. Plasmids were transformed into DH10Bac cells, and the desired clones were selected in a blue/white selection screen. Bacmid DNAs were transfected into Sf9 cells using FuGENE HD (Promega) according to the manufacturer's protocol. After three rounds of viral amplification in Sf9 cells, recombinant baculovirus was used to infect Sf9 cells. After baculovirus infection, the Sf9 cells were cultured for 12 hours at 27°C, followed by culture at 20°C. After 60 hours of infection, Sf9 cells were harvested and disrupted by sonication in 50 mM Tris-HCl (pH 8.0), 150 mM NaCl with 1 mM phenylmethylsulfonyl fluoride (PMSF), 5.2 µg/mL aprotinin, 2 µg/mL leupeptin and 1.4 µg/mL pepstatin A. After centrifugation, the supernatant was then ultracentrifuged at 40,000 rpm (Beckman Ti45 rotor) for 1 hour. The resulting membrane fraction was resuspended in solubilization buffer [50 mM Tris-HCl (pH 8.0), 150 mM NaCl, 20 mM imidazole, 2% DDM, 0.4% CHS, and 1 mM 2-mercaptoethanol] and incubated for 2 hours at 4°C. The debris was removed by another ultracentrifugation step (40,000 rpm, Beckman Ti45 rotor, 4°C, 1 hour), and the supernatant was loaded onto Ni-NTA agarose beads (QIAGEN). After the beads were washed with 20 mM Tris-HCl (pH 8.0), 300 mM NaCl, 0.05% DDM, 0.01% CHS, 1 mM 2-mercaptoethanol, and 40 mM imidazole, the protein was eluted with 20 mM Tris-HCl (pH 8.0), 300 mM NaCl, 0.05% DDM, 0.01% CHS, 1 mM 2-mercaptoethanol, and 300 mM imidazole. For MuTMC2, after the Ni-NTA affinity purification, the EGFP and His-tags were cleaved by TEV protease during dialysis at 4°C overnight against a buffer of 20 mM Tris-HCl (pH 8.0), 300 mM NaCl, 0.02% DDM, 0.004% CHS, and 2 mM dithiothreitol (DTT). The cleaved tags were removed by applying the digested sample to the Ni-NTA agarose beads and collecting the follow-through fractions. The TMC proteins were then applied to a Superose®6 increase 5/150 size-exclusion chromatography column (GE Healthcare, 29-0915-97) equilibrated with a buffer containing 20 mM HEPES-NaOH (pH 7.0), 150 mM NaCl, 0.05% DDM, 0.01% CHS and 2 mM DTT. The peak fractions were collected and concentrated to 2 mg/mL for EGFP-tagged CmTMC1 and 1 mg/mL for MuTMC2. The proteins were aliquoted and stored either in liquid nitrogen or at -80°C before use for electrophysiology. The purification procedure for EGFP was similar to that for EGFP-tagged CmTMC1 but without the ultracentrifugation step for the membrane preparation.

Mass spectrometry

The purified protein solution samples were subjected to mass spectrometry. The samples were dried and dissolved in 0.1% form-aldehyde before analysis using nano-RPLC (Easy-nLC 1000, Thermo Scientific). The nano-RPLC data obtained on an Orbitrap Elite mass spectrometer (Thermo Scientific) were searched using the TMC protein sequences and the UniProt *Spodoptera frugiperda* database.

Reconstitution of target proteins in liposomes

Purified proteins were incorporated into artificial liposomes, which were formed as previously described (Battle et al., 2009). Briefly, 200 µL of a 25 mg/mL solution of azolectin (Avanti Polar Lipids) in chloroform was dried under a stream of N₂ in a glass test tube while the tube was rotated to make a homogeneous lipid film. Once dried, 5 µL of pure water was added to the bottom (prehydration) followed by 1 mL of 0.4 M sucrose. The solution was incubated for 3 hours at 50°C until the lipid was resuspended. After the solution cooled to room temperature (21-24°C), the purified proteins were added to achieve the desired protein-to-lipid ratio (protein: lipid = 1:1000, wt: wt). The glass tube containing the protein-lipid solution was shaken gently on an orbital mixer for an additional 3 hours at 4°C. Care was taken when adding the protein to the sample to not disturb the lipid cloud. After this procedure, the sample was ready

to be used for the patch-clamp experiments. Confocal images were obtained in recording buffers using an Olympus FV1200 confocal microscope (Olympus Corporation, Tokyo, Japan) with a 60 × water-immersion objective lens, with excitation at 488 nm.

Patch-clamp recording

All recordings were performed with excised liposome patches. A previously reported protocol (Martinac et al., 2010) was used for the MscL channel recordings. For the TMC protein recordings, the pipette buffer contained 140 mM CsCl, 5 mM EGTA and 10 mM HEPES, which was adjusted with CsOH to pH 7.2, and the bath buffer contained 140 mM NaCl, 5 mM KCl, 2 mM MgCl₂ and 10 mM HEPES, which was adjusted with NaOH to pH 7.4. For recording in the NMDG-Cl or Na-gluconate solution, equimolar N-methyl-D-glucamine chloride (NMDG-Cl) and Na-gluconate, respectively, was used to replace NaCl in the bath solution and replace CsCl in the pipette solution. For the MgtE channel recordings, the pipette solution consisted of 210 mM N-methyl-D-glucamine, 90 mM MgCl₂, and 5 mM HEPES (pH 7.2), and the bath buffer contained 300 mM N-methyl-D-glucamine and 5 mM HEPES (pH 7.2). For the heat-denatured TMC protein recordings, the proteins were heat-denatured by being boiled at 95°C for 30 minutes. To assess the effect of the inhibitors, we first obtained a patch that showed normal channel openings. The inhibitors were then added to the bath solution to a certain concentration and the channel opening was recorded again from the same patch. The following inhibitors were tested: ruthenium red (RR, 140 μM), FM1-43 (3 μM), dihydrostreptomycin (DHS, 0.2 mM), amiloride (0.2 mM), benzamil (10 μM) and neomycin (1 mM). For pressure induced peak current and integrated current analysis, liposome patch was recorded at continuous 0 mmHg as baseline and use step pressures to induce current. For single-channel conductance analysis, to obtain single-channel activity of TMCs under pressure, we applied pressure continuously to the liposomes.

Borosilicate glass pipettes (BF150-86-10, Sutter Instrument) were pulled using a Flaming/Brown micropipette puller (P-97, Sutter Instrument) and polished to a diameter corresponding to a pipette resistance in the range of 4.0-6.0 MΩ. The patch resistance increased to ~2 GΩ after the pipette formed a tight seal with the liposome membrane. Negative pressure was applied to the excised membrane patches via an HSPC (ALA-scientific). Signals generated from HEKA software were sent to the HSPC to control the timing and intensity of the pressure. All experiments were performed at room temperature (21-24°C), and the data were acquired at 50 kHz with a 0.5-kHz low-pass filter and 50-Hz notch filter using an EPC-10 amplifier and Pulse software (HEKA Electronic, Lambrecht, Germany). All of the independent recordings are from different reconstitutions. For spontaneous activity of TMC proteins, after we got stable recording, a new recording was obtained separately about 10 s for further analysis.

QUANTIFICATION AND STATISTICAL ANALYSIS

The current-voltage (I-V) curves of the spontaneous and mechanosensitive currents were plotted and fitted to the response amplitude measured from -120 to +120 mV in 40-mV increments. The single-channel conductance was obtained through linear fitting of the current-voltage plots. For quantitative analysis, the Pulse files were converted into PCLAMP format using the ABF File Utility, Ver. 2.1.75 (Synaptosoft, Decatur, GA). Current traces analysis and fits were done with Clampfit 10.4 (Axon Instruments, Foster City, CA). The Statistical Program for Social Sciences (SPSS) 22.0 (IBM Inc.) and GraphPad Prism 7 (GraphPad Software) were used for statistical analysis and graph generation. t test and one-way ANOVA were used to assess statistical significance. The data are shown as the mean value ± s.e.m.

DATA AND CODE AVAILABILITY

Datasets related to this article can be found at <https://doi.org/10.17632/mcswwckj5wd.1>, an open-source online data repository hosted at Mendeley Data.